NUCL SCI TECH (2020) 31:119
https://doi.org/10.1007/s41365-020-00827-1

Studies on mass attenuation coefficients for some body tissues with different medical sources and their validation using Monte Carlo codes

Sepideh Yazdani Darki[1] · Sajad Keshavarz[2]

Received: 26 July 2020 / Revised: 18 October 2020 / Accepted: 22 October 2020 / Published online: 4 December 2020

Abstract The mass attenuation coefficients of the breasts, lungs, kidneys, pancreas, liver, eye lenses, thyroid, brain, ovary, heart, large intestines, blood, skin, spleen, muscle, and cortical bone were measured at different sources (i.e., 0.021, 0.029, 0.03, 0.14, 0.218, 0.38, 0.412, 0.663, 0.83, and 1.25 MeV) using various methods including the Monte Carlo N-particle transport code (MCNP), the geometry and tracking code (GEANT4), and theoretical approach described in this study. Mass attenuation coefficients were also compared with the values from the national institute of standards and technology (NIST-XCOM). The values obtained were similar to those obtained using NIST-XCOM. Our results show that the theoretical method is quite convenient in comparison with GEANT4 and MCNP in the calculation of the mass attenuation coefficients of the human body samples applied when compared with the NIST values and demonstrated an acceptable difference.

Keywords Mass attenuation coefficient · MCNP · Geant4 · XCOM · Human organs

1 Introduction

Many sources are used in medicine to diagnose and treat different abnormalities and cancers. Using these sources can be helpful for determining the rate of attenuation in each organ. In this study, sources that have more applications in various types of diagnosis and treatment have been studied. To treat prostate cancer, palladium-103 with an average photon energy of 0.021 MeV has been used [1, 2]. In addition, Cs-137 source (mean energy = 0.030 MeV) has been applied to intracavitary brachytherapy [3–5]. Moreover, Ba-133 has been used in dose distribution measurements at distances that range from very close up to the brachytherapy source [6], and Ir-192 with a 0.380 MeV mean photon energy is used in brachytherapy with a high dose rate [7–9]. The intra-articular injection of Au-198 (mean photon energy = 0.412 MeV) has been used to treat repeated hemarthrosis of the elbows, knees, or ankles, which reduces the incidence of hemarthrosis and slows the rate of evolution of radiographic changes [10, 11]. In addition, Co-60 and Cs-137 are used for the measurement and calculation of the dose at long distances when applying brachytherapy [12–14], and radium-226 is used for the treatment of cervical and endometrial cancer. However, radium-226 is a dangerous material, and other sources are being applied as a replacement [15]. In addition, technetium-99 m (mean photon energy = 0.14 MeV) compounds are being used in the imaging of heart muscle perfusion [16]. The use of iodine 125 diagnostic kits for radioimmunoassay (RIA) measurements in conventional medical diagnostic laboratories is common. Iodine 125 emits gamma and X-rays with a mean energy of 0.029 MeV [17]. When a photon moves through matter, it may interact through any of the three major interactions: Compton, photoelectric, and pair production based on their energy [18].

When a beam of gamma rays passes through matter, the absorption and scattering of the primary photons are called attenuation [19]. Mass attenuation coefficients provide

✉ Sajad Keshavarz
sajadkeshavarz7@gmail.com

[1] Department of Physics, University of Yazd, Yazd, Iran

[2] Department of Medical Radiation Engineering, University of Science and Research Branch Tehran, Tehran, Iran

essential data on various fields, such as the elemental concentration or biological composition, nuclear medicine, medical applications, and radiation dosimetry. In the biological and medical contexts, the mass attenuation coefficient is a key parameter for various dosimetry materials [20, 21]. When photons deposit their energy in tissues, the radiation dose can be estimated based on the mass attenuation coefficients, particularly in the human body [20]. The calculations of the mass attenuation coefficients are based on the Beer–Lambert law:

$$I = I_0 \mathrm{e}^{-\mu x}, \tag{1}$$

where I_0 and I are the initial (before the sample) and final (after the model) photon intensities, respectively, and x is the thickness of the material. The mass attenuation coefficient $\mu_\mathrm{m} = \mu/\rho$ is the slope of a straight-line equation [22, 23].

There have been many articles on the mass attenuation coefficient in various tissues of the human body. In Ref. [23], Arslan investigated the mass attenuation coefficients, effective atomic numbers, effective electron densities, and Kerma relative to air for muscle, bone, and adipose tissues within a photon energy region of 20 keV to 50 MeV using the Geant4 simulation package and theoretical calculations and compared the values of the Auto-Zeff program with the results of other studies. The authors of Ref. [21] calculated the mass attenuation coefficient (μ/ρ), mass energy absorption coefficient (μ_en/ρ), and effective atomic number (Z_eff) in different tissues of human organs using a pocket formula. The new chemical formula was assigned in Ref. [21] for all tissues studied based on their composition.

Tissue-equivalent phantoms are valuable for experimental biomedical research because they can provide a good simulation of real human tissue, and aid in the development and validation of the modalities in medical applications [24]. Many research groups have recently measured the mass attenuation coefficients using Monte Carlo simulation models in different materials and have obtained the successful results. Ermis et al. [19] used various theoretical methods to determine the mass attenuation coefficient of other tissues. Their results show that calculating the mass attenuation coefficient with the FLUKA code is more appropriate than the GEANT4 code when compared with NIST values at 60, 80, and 150 keV of photon energy. The percentage difference between the mass density of each material and each organ tissue was evaluated by Alssabbagh et al. [25], who compared the mass attenuation coefficient and density for nine 3D printing materials as tissue-equivalent materials using the NIST-XCOM database, and the X-ray attenuation properties of nine different human organ tissues using the values listed in the International Commission on Radiation Units and Measurements (ICRU), report 44. These results showed that we can use 3D wood material to create and simulate human phantoms. El-Khayatt et al. [26] analyzed tissue-equivalent materials for use as human brain tissue substitutes in dosimetry for diagnostic radiology and calculated the total mass attenuation coefficients, absorbed dose, and mass energy-absorption coefficient for bolus, nylon, orange articulation wax, red articulation wax paraffin, and water. The results have shown that water is the best material for the brain among the other materials that were investigated.

The study of the mass attenuation coefficient in different tissues of human organs plays a vital role in radiotherapy and medical diagnosis. It is difficult to measure the basic photon interaction parameters in the tissues of human organs because many chemical and biological reactions take place simultaneously. Thus, there is a need to estimate these parameters theoretically. Hence, in the present study, we considered the mass attenuation coefficient of many tissues of human organs (blood, brain, breasts, spleen, eye lenses, heart, liver, lungs, muscle, ovaries, pancreas, skin, thyroid, kidneys, cortical bone, and large intestines) within the mean photon energy range of 0.021–1.25 MeV.

In previous studies, fewer organs and fewer sources were used. However, in this study, even more organs and more sources were used and were also prevented by receiving doses from other tissues in medicine, particularly tissues that are close to each other. This causes secondary cancers in other organs, which can be reduced by knowing the mass attenuation coefficient of each organ. Because a direct measurement of the attenuation coefficient is not easily possible using a simulation, the desired results can be achieved more quickly before conducting clinical studies.

2 Materials and methods

The chemical composition, weight fractions, tissue densities, and tissue equivalents have been studied in this present study, which are listed in Table 1. These values are used from the ICRU Report 44 [27], which are referenced data providing the required mass attenuation coefficient calculations.

2.1 Theoretical method

When a photon moves through matter, it may interact through any of the three significant interactions: Compton, photoelectric, and pair production based on their energy [18]. There are other interactions that are not crucial for photon interactions.

Table 1 Components of element organs

Materials	Density (g/cm^3)	Weight fraction (%)												
		H	C	N	O	Na	P	S	Cl	K	Ca	Fe	Mg	I
Breast	1.02	0.106	0.332	0.03	0.527	0.001	0.001	0.002	0.001	–	–	–	–	–
Lung	1.05	0.103	0.105	0.031	0.749	0.002	0.002	0.003	0.003	0.002	–	–	–	–
Kidney	1.05	0.103	0.132	0.03	0.724	0.002	0.002	0.002	0.002	0.002	0.001	–	–	–
Pancreas	1.04	0.106	0.169	0.022	0.694	0.002	0.002	0.001	0.002	0.002	0.001	–	–	–
Liver	1.06	0.102	0.139	0.03	0.716	0.002	0.003	0.003	0.002	0.003	–	–	–	–
Eye Lens	1.07	0.096	0.195	0.057	0.646	0.001	0.001	0.003	0.001	0.002	0.001	–	–	–
Thyroid	1.05	0.104	0.119	0.024	0.746	0.002	0.001	0.001	0.002	0.001	–	–	–	0.001
Brain	1.04	0.107	0.145	0.022	0.712	0.002	0.004	0.002	0.003	0.003	–	–	–	–
Ovary	1.05	0.105	0.093	0.024	0.768	0.002	0.002	0.002	0.002	0.002	–	–	–	–
Heart	1.06	0.103	0.121	0.032	0.734	0.001	0.001	0.002	0.003	0.002	–	0.001	–	–
Large intestine	1.03	0.106	0.115	0.022	0.751	0.001	0.001	0.001	0.002	0.001	–	–	–	–
Blood	1.06	0.102	0.110	0.033	0.745	0.001	0.001	0.002	0.003	0.002	–	0.001	–	–
Skin	1.09	0.100	0.204	0.042	0.645	0.002	0.001	0.002	0.003	0.001	–	–	–	–
Spleen	1.06	0.103	0.113	0.032	0.741	0.001	0.003	0.002	0.002	0.003	–	–	–	–
Muscle (Skeletal)	1.05	0.102	0.143	0.034	0.710	0.001	0.002	0.003	0.001	0.004	–	–	–	–
Cortical bone	1.92	0.034	0.165	0.042	0.435	0.001	0.103	0.003	–	–	0.225	–	0.002	–

The probability of the total interaction, which is called the linear attenuation coefficient (μ), is shown in Eq. (2) [28]:

$$\mu\left(\mathrm{cm}^{-1}\right) = \sigma_{\text{Compton}} + \sigma_{\text{photo electrice}} + \sigma_{\text{pair production}}, \quad (2)$$

$$\sigma_{\text{photo electrice}} = cN\left(\frac{z^b}{E_\gamma^a}\right)[1 - f(Z)], \quad (3)$$

$$\sigma_{\text{Compton}} = NZ\,f\left(E_\gamma\right), \quad (4)$$

$$\sigma_{\text{pair production}} = NZ^2 f\left(E_\gamma, Z\right), \quad (5)$$

where c is a constant coefficient, independent of Z and E_γ., parameters a and b are constants with values of between 3 and 5 depending on the gamma energy, N is the nuclear density, and Z is the atomic number [28].

As a result,

$$\mu_{\text{m}}\left(\mathrm{cm}^2/\mathrm{g}\right) = \frac{\mu(\mathrm{cm}^{-1})}{\rho\left(^{\mathrm{g}}/_{\mathrm{cm}^3}\right)}, \quad (6)$$

where μ_{m} is the mass attenuation coefficient and ρ is the density. Using the definitions of the photoelectric, Compton, and pair production cross sections, we calculated the value of the linear attenuation coefficient. There are many tables in which the mass attenuation coefficient has been calculated for all elements and at greater photon energy, which those listed in the tables in Ref. [29].

The total mass attenuation coefficient for a compound will be calculated by combining Eq. (6) and the weight action (%wt) for every element in the compound, as shown in Eq. (7):

$$\mu_{\text{c}}\left(\mathrm{cm}^2/\mathrm{g}\right) = \sum_i w_i \times \mu_{\text{m}i}, \quad (7)$$

where μ_{c}, w_i and μ_{m_i} are the total mass attenuation coefficient of a compound, weight fraction, and mass attenuation coefficient for every element, respectively [30].

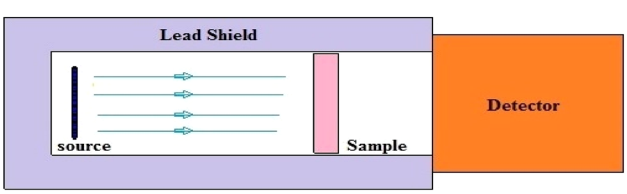

Fig. 1 (Color online) Sketch of simulated geometry in MCNP

2.2 MCNP simulation

A Monte Carlo simulation is a general-purpose tool for studying the interaction of X and gamma rays, neutrons, and electrons with matter owing to the comprehensive applications of the Monte Carlo N-particle transport code (MCNPX) in medical and medical radiation investigations. This comparative study can use a unified database on the mass attenuation coefficients of the materials [12]. The composition and density of the samples used are presented in Table 1.

In this study, MCNPX was used to calculate the attenuation properties of human body organs. MCNPX is a radiation transport code for modeling and calculating the

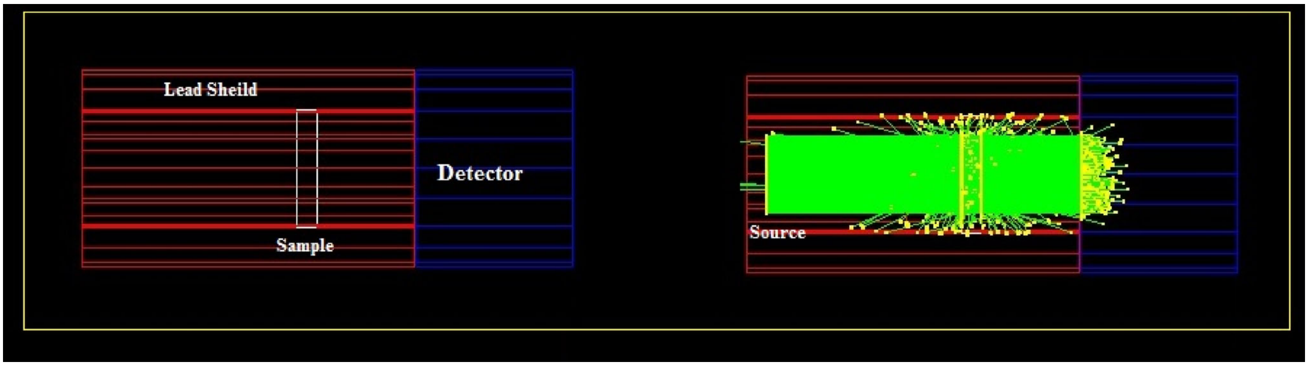

Fig. 2 (Color online) Sketch of simulated geometry in GEANT4

interaction of radiation with materials and tracking all particles at different energies. When a photon passes through a material, it loses its energy through well-known processes such as Compton scattering, photoelectric effects, and pair production [31]. Blood, brain, breast, spleen, eye lens, heart, liver, lung, muscle, ovary, pancreas, skin, thyroid, kidney, cortical bone, and large intestine materials, with a radius of 3 cm and height of 1 cm, as sketched in Fig. 1, were selected to investigate the photon attenuation.

Table 2 Calculated mass attenuation coefficient and percentage difference among standard XCOM data with MCNPX, Geant4, and the theoretical method (%) for breast and blood

Nuclide	Mean-energy (MeV)	Mass attenuation coefficient of breast				Percentage difference (%) for breast		
		MCNP	GAENT4	Theoretical	XCOM	MCNP	GAENT4	Theoretical
Pd-103	0.021	0.63446	0.62547	0.62024	0.6214	2.058	0.650	0.187
I-125	0.029	0.35881	0.36692	0.34431	0.3561	0.755	2.948	3.424
Cs-131	0.030	0.35745	0.36511	0.33357	0.3403	4.797	6.795	2.017
Tc-99 m	0.140	0.15242	0.16275	0.16448	0.1525	0.052	6.298	7.283
Ba-133	0.218	0.13001	0.13657	0.13517	0.1322	1.684	3.199	2.197
Ir-192	0.380	0.10093	0.10688	0.10358	0.1077	6.707	0.767	3.977
Au-198	0.412	0.09991	0.10328	0.10342	0.1043	4.393	0.987	0.850
Cs-137	0.663	0.08344	0.08692	0.08693	0.0852	2.109	1.978	1.990
Ra-226	0.830	0.07492	0.07135	0.07417	0.07686	2.589	7.722	3.626
Co-60	1.25	0.06197	0.06897	0.06409	0.06287	1.452	8.844	1.903
Nuclide	Mean-energy (MeV)	Mass attenuation coefficient of blood				Percentage difference (%) for blood		
		MCNP	GAENT4	Theoretical	XCOM	MCNP	GAENT4	Theoretical
Pd-103	0.74778	0.74778	0.74357	0.75083	0.73420	1.816	1.26	2.214
I-125	0.40588	0.40588	0.39172	0.41101	0.39790	1.966	1.577	3.189
Cs-131	0.38372	0.38372	0.40445	0.37009	0.37790	1.516	6.564	2.11
Tc-99 m	0.15102	0.15102	0.16444	0.15082	0.15250	0.98	7.261	1.113
Ba-133	0.13025	0.13025	0.14518	0.14000	0.13180	1.19	9.216	5.857
Ir-192	0.10083	0.10083	0.11408	0.10375	0.10730	6.416	5.943	3.421
Au-198	0.09887	0.09887	0.10631	0.10358	0.10390	5.087	2.266	0.308
Cs-137	0.08293	0.08293	0.08734	0.08838	0.08491	2.387	2.782	3.926
Ra-226	0.07514	0.07514	0.07333	0.07554	0.07661	1.956	4.472	1.416
Co-60	0.06132	0.06132	0.06028	0.06637	0.06266	2.185	3.948	5.589

Table 3 Calculated mass attenuation coefficient and percentage difference among standard XCOM data with MCNPX, Geant4, and theoretical methods (%) of skin and lung

Nuclide	Mean-energy (MeV)	Mass attenuation coefficient of skin				Percentage difference (%) for skin		
		MCNP	GAENT4	Theoretical	XCOM	MCNP	GAENT4	Theoretical
Pd-103	0.021	0.69821	0.69851	0.68247	0.68950	1.247	1.289	1.03
I-125	0.029	0.39068	0.37823	0.39496	0.38100	2.477	0.732	3.534
Cs-131	0.030	0.37193	0.35793	0.35732	0.36260	2.508	1.304	1.477
Tc-99 m	0.140	0.15450	0.16306	0.15511	0.15200	1.618	6.782	2.005
Ba-133	0.218	0.13001	0.13873	0.14368	0.13150	1.146	5.211	8.477
Ir-192	0.380	0.10045	0.10051	0.10383	0.10710	6.62	6.556	3.149
Au-198	0.412	0.09881	0.10107	0.10366	0.10370	4.948	2.602	0.038
Cs-137	0.663	0.08297	0.09377	0.08894	0.08475	2.145	9.619	4.711
Ra-226	0.830	0.07599	0.07111	0.07602	0.07646	0.618	7.523	0.578
Co-60	1.25	0.06149	0.06255	0.06212	0.06254	1.707	0.0159	0.676
Nuclide	Mean-energy (MeV)	Mass attenuation coefficient of lungs				Percentage difference (%) for lungs		
		MCNP	GAENT4	Theoretical	XCOM	MCNP	GAENT4	Theoretical
Pd-103	0.021	0.75502	0.75290	0.73259	0.74430	1.419	1.142	1.598
I-125	0.029	0.40779	0.39464	0.40241	0.40180	1.468	1.814	0.151
Cs-131	0.030	0.38470	0.39131	0.37268	0.38150	0.831	2.506	2.366
Tc-99 m	0.140	0.15354	0.16427	0.16934	0.15260	0.612	7.104	9.885
Ba-133	0.218	0.12996	0.14221	0.13879	0.13200	1.569	7.179	4.892
Ir-192	0.380	0.10579	0.10108	0.10373	0.10740	1.521	6.252	3.538
Au-198	0.412	0.10001	0.10522	0.10356	0.10400	3.989	1.159	0.424
Cs-137	0.663	0.07253	0.09717	0.08195	0.08498	17.165	12.545	3.697
Ra-226	0.830	0.07502	0.08503	0.07537	0.07667	2.199	9.831	1.724
Co-60	1.25	0.06105	0.06313	0.06580	0.06271	2.719	0.665	4.696

MCNPX simulation parameters (cards) such as cell, surface, and material descriptions, the position of each tool, and the definitions and features of the sources are defined in the input file according to their properties [32].

The geometry of the sample was defined as a cylinder with a 1 cm thickness (height) and a radius of 3 cm. A schematic view of the MCNP-X simulation setup with a lead (Pb) collimator, investigated for sample organs and detection areas with defined geometries in the MCNP-X input file, is presented in Fig. 1.

The geometry includes a gamma-ray source, lead collimators, samples, and detection areas that have been defined in the cell card, surface card, and data card sections of the MCNP input by considering different variables such as CEL, ERG, DIR, POS, and PAR. The geometric center of the detection area was considered for the location of the plating source. The source has been defined with mean photon energies of 0.021, 0.029, 0.03, 0.14, 0.218, 0.38, 0.412, 0.663, 0.83, and 1.25 MeV.

In addition, the sample was located 10 cm away from the source, and the detector was found in a 5 cm model. A lead shield surrounded the sample and source. Tally F2 was used to obtain the MCNP simulation data. This tally calculates the flux on the detector for every energy source. The MCNP sources were simulated as a circle surface using different photon energies for every source. Simulations were conducted using 5×10^7 histories, and all simulation data were reported to have less than 1% error.

2.3 Geant4 simulation

The determination of the mass attenuation coefficient for soft tissues and tissue substitute materials given in Table 1 by the Geant4 simulation code was achieved by writing C++ types [33] depending on the object-oriented programming concept. The model was written using three mandatory classes: First, the geometry of the model defined in detector construction and the physics process, which

Table 4 Calculated mass attenuation coefficient and percentage difference among standard XCOM data with MCNPX, Geant4, and theoretical methods (%) of kidneys and pancreas

Nuclide	Mean-energy (MeV)	Mass attenuation coefficient of kidneys				Percentage difference (%) for kidneys		
		MCNP	GAENT4	Theoretical	XCOM	MCNP	GAENT4	Theoretical
Pd-103	0.021	0.74399	0.73916	0.72274	0.73430	1.302	0.657	1.599
I-125	0.029	0.40380	0.38201	0.39871	0.39820	1.386	4.238	0.127
Cs-131	0.030	0.38147	0.39251	0.37975	0.37820	0.857	3.645	0.408
Tc-99 m	0.140	0.15359	0.16914	0.16927	0.15260	0.644	9.778	9.848
Ba-133	0.218	0.13064	0.12391	0.13880	0.13200	1.041	6.528	4.899
Ir-192	0.380	0.10573	0.10363	0.10372	0.10740	1.579	3.637	3.548
Au-198	0.412	0.10999	0.10498	0.10355	0.10400	5.445	0.933	0.434
Cs-137	0.663	0.08335	0.09204	0.08119	0.08498	1.955	7.67	4.668
Ra-226	0.830	0.07507	0.07785	0.07529	0.07667	2.131	1.515	1.832
Co-60	1.25	0.06094	0.06552	0.06580	0.06271	2.904	4.288	4.696
Nuclide	Mean-energy (MeV)	Mass attenuation coefficient of pancreas				Percentage difference (%) for pancreas		
		MCNP	GAENT4	Theoretical	XCOM	MCNP	GAENT4	Theoretical
Pd-103	0.021	0.72288	0.72821	0.71861	0.71630	0.91	1.635	0.321
I-125	0.029	0.40275	0.38353	0.38870	0.39180	2.718	2.156	0.797
Cs-131	0.030	0.38035	0.38917	0.37150	0.37250	2.063	4.283	0.269
Tc-99 m	0.140	0.15626	0.16129	0.16817	0.15290	2.15	5.201	9.08
Ba-133	0.218	0.13039	0.13850	0.13796	0.13230	1.464	4.476	4.102
Ir-192	0.380	0.10068	0.10827	0.10369	0.10770	6.972	0.526	3.867
Au-198	0.412	0.10994	0.10361	0.10352	0.10430	5.13	0.665	0.753
Cs-137	0.663	0.08468	0.07415	0.08785	0.08520	0.614	14.902	3.016
Ra-226	0.830	0.07781	0.07616	0.07504	0.07687	1.208	0.932	2.438
Co-60	1.25	0.06232	0.05345	0.06432	0.06287	0.882	17.623	2.254

were coded in the physics list, were used. Finally, the primary generator action, which is one of the few mandatory classes that need to be set up, was used to define the primary events and particles that are to be propagated through the simulation geometry. The physics of the simulation are based on a narrow beam geometry with various photon energies according to the mass attenuation coefficient. The mean energy of the incident photons varied between 0.021 and 1.25 MeV. To calculate the mass attenuation coefficients in relevant physical processes such as the photoelectric effect, Compton scattering and pair production were used. Geant4 electromagnetic physics processes have been successfully compared with the National Institute of Standards and Technologies (NIST) reference data. The simulated geometry and source are shown in Fig. 2.

This allows users to define classes for the detector geometry, primary particle generator, and physics processes to handle the interactions of particles with matter. It provides a set of electromagnetic physics processes driving the photon–tissue interactions (photoelectric effect, Compton scattering, Rayleigh scattering, and pair production) over a wide range of energy [23].

2.4 XCOM program

The mass attenuation coefficient values of tissues and tissue-equivalent materials were calculated using the XCOM program. XCOM is a program that generates mass attenuation coefficient elements, compounds, and mixtures for desired energies of 1 keV up to 100 GeV, and this program can generate cross sections under standard energy

Table 5 Calculated mass attenuation coefficient and percentage difference among standard XCOM data with MCNPX, Geant4, and theoretical methods (%) of liver and thyroid

Nuclide	Mean-energy (MeV)	Mass attenuation coefficient of liver				Percentage difference (%) for liver		
		MCNP	GAENT4	Theoretical	XCOM	MCNP	GAENT4	Theoretical
Pd-103	0.021	0.74979	0.74769	0.73256	0.73920	1.412	1.135	0.906
I-125	0.029	0.40841	0.38750	0.40450	0.39990	2.083	3.2	1.137
Cs-131	0.030	0.38627	0.39151	0.36549	0.37980	1.674	2.99	3.915
Tc-99 m	0.140	0.15100	0.16853	0.15075	0.15250	0.993	9.511	1.16
Ba-133	0.218	0.13015	0.13495	0.13999	0.13180	1.267	2.334	5.85
Ir-192	0.380	0.10610	0.10275	0.10376	0.10730	1.131	4.428	3.411
Au-198	0.412	0.10999	0.10213	0.10360	0.10390	5.536	1.733	0.289
Cs-137	0.663	0.07215	0.08243	0.08469	0.08490	17.671	2.996	0.247
Ra-226	0.830	0.07511	0.07364	0.07561	0.07660	1.983	4.019	1.309
Co-60	1.25	0.06337	0.06956	0.06637	0.06265	1.136	9.933	5.604
Nuclide	Mean-energy (MeV)	Mass attenuation coefficient of thyroid				Percentage difference (%) for thyroid		
		MCNP	GAENT4	Theoretical	XCOM	MCNP	GAENT4	Theoretical
Pd-103	0.021	0.74203	0.72400	0.72088	0.73320	1.189	1.27	1.709
I-125	0.029	0.40712	0.37700	0.39875	0.39850	2.117	5.702	0.062
Cs-131	0.030	0.38462	0.39719	0.37926	0.37860	1.565	4.68	0.174
Tc-99 m	0.140	0.15281	0.16145	0.15029	0.15330	0.32	5.048	2.002
Ba-133	0.218	0.13059	0.13950	0.13922	0.13220	1.232	5.232	5.042
Ir-192	0.380	0.10573	0.10894	0.10371	0.10750	1.674	1.321	3.654
Au-198	0.412	0.10024	0.10776	0.10354	0.10410	3.85	3.396	0.54
Cs-137	0.663	0.06182	0.06959	0.08014	0.08505	37.576	22.215	6.126
Ra-226	0.830	0.07625	0.08344	0.07520	0.07673	0.629	8.041	2.034
Co-60	1.25	0.06337	0.06585	0.06592	0.06276	0.962	4.692	4.793

or a grid selected by the user [30]. In addition, it provides a total cross section for processes such as incoherent and coherent scattering, photoelectric absorption, and pair production from the atomic nucleus. In this program, we used the ICRU report 44 for the components of the organs and used different photon energies of the sources for calculating the mass attenuation coefficient [19, 20].

3 Results and discussion

3.1 Total mass attenuation coefficient

By using Tables 2, 3, 4, 5, 6, 7, 8, 9 and inserting the weight fraction of each material and human organ into the web version of XCOM software, MCNP, Geant4, and the theoretical method, the total mass attenuation coefficient and percentage difference were calculated for the mean photon energy range of 0.21 to 1.25 MeV, for which most of the medical applications fall within this energy interval and sources. The total mass attenuation coefficient decreases proportionally with the number of X-ray photon interactions with the materials for this energy range. In Figs. 3, 4, 5, 6, 7, 8, 9, 10, the calculated mass attenuation coefficients versus the mean photon energies of each absorber material are shown. A comparison of the results from the programs can be seen in these figures and tables.

In the low-energy region, the calculated mass attenuation coefficients were less than those of Geant4 and MCNPX when compared to the XCOM values, as can be seen in Figs. 3, 4, 5, 6, 7, 8, 9, 10. The differences in attenuation values can be due to different models in the Monte Carlo codes. Fundamentally, both MC codes use the Evaluated Photon Data Library (EPDL), which is mostly related to the NIST standard reference data products [19].

The theoretical results are in excellent agreement with the XCOM program. However, the values of Geant4 and MCNPX show extremely little difference from both academic and XCOM costs. The discrepancy between these results could be due to the scattering of radiation around

Table 6 Calculated mass attenuation coefficient and percentage difference among standard XCOM data with MCNPX, Geant4, and theoretical methods (%) of brain and eye lens

Nuclide	Mean-energy (MeV)	Mass attenuation coefficient of brain				Percentage difference (%) for brain		
		MCNP	GAENT4	Theoretical	XCOM	MCNP	GAENT4	Theoretical
Pd-103	0.021	0.75250	0.74792	0.74305	0.74150	1.461	0.858	0.208
I-125	0.029	0.41159	0.39012	0.39857	0.40130	2.5	2.865	0.684
Cs-131	0.030	0.38829	0.39598	0.38014	0.38110	1.851	3.757	0.252
Tc-99 m	0.140	0.15329	0.16265	0.15827	0.15310	0.123	5.871	3.266
Ba-133	0.218	0.13076	0.13033	0.13796	0.13240	1.254	1.588	4.03
Ir-192	0.380	0.10611	0.10221	0.10371	0.10780	1.592	5.469	3.943
Au-198	0.412	0.10032	0.11945	0.10355	0.10440	4.066	12.599	0.82
Cs-137	0.663	0.09637	0.07250	0.08073	0.08527	11.518	17.613	5.623
Ra-226	0.830	0.07673	0.08530	0.07524	0.07694	0.273	9.8	2.259
Co-60	1.25	0.06368	0.06249	0.06540	0.06293	1.177	0.704	3.776
Nuclide	Mean-energy (MeV)	Mass attenuation coefficient of eye lens				Percentage difference (%) for eye lens		
		MCNP	GAENT4	Theoretical	XCOM	MCNP	GAENT4	Theoretical
Pd-103	0.021	0.67638	0.65354	0.70630	0.70280	3.906	7.537	0.495
I-125	0.029	0.38203	0.35979	0.39420	0.38570	0.96	7.201	2.156
Cs-131	0.030	0.36090	0.37438	0.35676	0.36680	1.634	2.024	2.814
Tc-99 m	0.140	0.15095	0.17993	0.15177	0.15150	0.364	15.8	0.177
Ba-133	0.218	0.12911	0.15047	0.14095	0.13110	1.541	12.873	6.988
Ir-192	0.380	0.10597	0.11360	0.10377	0.10670	0.688	6.073	2.823
Au-198	0.412	0.10997	0.10200	0.10360	0.10330	6.065	1.274	0.289
Cs-137	0.663	0.07155	0.07540	0.08477	0.08443	18.001	11.976	0.401
Ra-226	0.830	0.07586	0.07664	0.07561	0.07617	0.408	0.613	0.74
Co-60	1.25	0.06280	0.06694	0.06682	0.06230	0.796	6.931	6.764

and not reaching the detector and the random process of the Monte Carlo method [20].

As shown in Tables 2, 3, 4, 5, 6, 7, 8, 9, it can be noted that the lowest standard deviation rates were obtained for the theoretical data as compared to XCOM. It was observed that the photon attenuation parameter of each sample decreased with enhanced photon energy owing to the increased penetration of the photons from the attenuator. In low-energy regions, the MCNPX and GEANT4 results are closer to each other than they are with the theoretical products. This result indicates that MCNPX may be a more suitable program for live biological media investigations in low-energy regions. In addition, MCNPX has extensive cross-sectional libraries for low-energy areas. The results also show that MCNPX and GEANT4 within the range of low, medium, and high energy can differ because these codes have been used for other physical models. The mass attenuation coefficients of human body organs are comparable with the theoretical and standard NIST results [32].

To analyze and compare the percentage difference among XCOM data, MCNPX, the Geant4 programs, and the theoretical approach, we calculated the deviations among these methods (Tables 2, 3, 4, 5, 6, 7, 8, 9). The percentage difference was calculated using the formula ($D = (E_a - E_b)/E_b \times 100\%$). In this formula, E_a is the first result and E_b is the second result in calculating the percentage difference between two values.

The mass attenuation coefficient (μ/ρ) values of tissues within the mean photon energy range of 21 keV to 1.25 meV are listed in Tables 2, 3, 4, 5, 6, 7, 8, 9. The μ/ρ values of the tissues vary significantly between different energy regions. Within the low-energy region, the variation is quite broad, is merely due to a photoelectric effect, and sharply increases and decreases along with the changes in the energy levels. This is natural because the interaction between the cross section is dependent on the photon energy and atomic number. However, Compton scattering becomes a dominant incident within the medium-energy region as the interaction between the cross section is independent of the photon energy, whereas it is largely dependent upon the atomic number. The MCNPX and Geant4 simulated mass attenuation coefficients for tissues

Table 7 Calculated mass attenuation coefficient and percentage difference among standard XCOM data with MCNPX, Geant4, and theoretical methods (%) of heart and large intestine

Nuclide	Mean-energy (MeV)	Mass attenuation coefficient of heart				Percentage difference (%) for heart		
		MCNP	GAENT4	Theoretical	XCOM	MCNP	GAENT4	Theoretical
Pd-103	0.021	0.74409	0.75111	0.74671	0.75000	0.794	0.147	0.44
I-125	0.029	0.40718	0.40232	0.40954	0.40440	0.682	0.517	1.255
Cs-131	0.030	0.38481	0.39201	0.38953	0.38390	0.236	2.068	1.445
Tc-99 m	0.140	0.15112	0.16892	0.15095	0.15260	0.979	9.661	1.093
Ba-133	0.218	0.13026	0.13568	0.13013	0.13200	1.335	2.712	1.437
Ir-192	0.380	0.10641	0.10696	0.10375	0.10740	0.93	0.411	3.518
Au-198	0.412	0.10999	0.10649	0.10359	0.10400	5.445	2.338	0.395
Cs-137	0.663	0.08471	0.09429	0.08839	0.08498	0.318	9.873	3.857
Ra-226	0.830	0.07546	0.08371	0.07654	0.07667	1.603	8.409	0.169
Co-60	1.25	0.06326	0.07318	0.06429	0.06271	0.869	14.307	2.457
Nuclide	Mean-energy (MeV)	Mass attenuation coefficient of large intestine				Percentage difference (%) for large intestine		
		MCNP	GAENT4	Theoretical	XCOM	MCNP	GAENT4	Theoretical
Pd-103	0.021	0.71729	0.68561	0.70400	0.70570	1.615	2.93	0.241
I-125	0.029	0.39928	0.38402	0.38168	0.38750	2.95	0.906	1.524
Cs-131	0.030	0.37632	0.38403	0.36465	0.36860	2.051	4.017	1.083
Tc-99 m	0.140	0.15207	0.16131	0.15644	0.15290	0.545	5.213	2.262
Ba-133	0.218	0.13067	0.13920	0.13651	0.13230	1.247	4.956	3.084
Ir-192	0.380	0.10608	0.10731	0.10363	0.10770	1.527	0.363	3.927
Au-198	0.412	0.11912	0.10272	0.10347	0.10430	12.441	1.538	0.802
Cs-137	0.663	0.09262	0.09329	0.08744	0.08523	7.978	8.639	2.527
Ra-226	0.830	0.07573	0.08463	0.07469	0.07690	1.544	9.133	2.958
Co-60	1.25	0.06111	0.06903	0.06473	0.06289	2.912	8.894	2.842

were comparable with the theoretical XCOM values and theoretical data. It can be concluded that the mass attenuation coefficients for tissues having low and high atomic number elements for low- to high-energy photons were found to be comparable with the experiment and GEANT-4 results, as well as the MCNP simulation codes. The present study will be beneficial for developing materials with different energy levels for radiation dosimetry and medical and nuclear technologies.

According to the results obtained from Tables 2, 3, 4, 5, 6, 7, 8, 9, with increasing energy, the mass attenuation coefficient decreased for all tissues. Whereas the cortical bone has the highest mass attenuation, the breast has the least mass attenuation. In other words, bone tissue has a higher attenuation coefficient than the other organs because of its higher atomic number and density, and breast tissue, owing to its lower density, has a lower mass attenuation coefficient than the other organs. The increase in mass attenuation is related to the inverse of energy and directly related to the density.

The percentage differences were calculated for each simulation code separately. As observed in Tables 2, 3, 4, 5, 6, 7, 8, 9, the theoretical and Geant4 methods had mostly similar deviations for the investigated organs. It can be concluded that each Monte Carlo code has different capabilities in different energy regions. In the low-energy area, the standard deviation rates of theoretical and Geant4 were less than those of MCNPX.

Ermis et al. [19] and Huseyin et al. [34] measured the mass attenuation coefficients of different parts of the human body using Monte Carlo methods, and the results were in good agreement with the results of their study on the calculation of the mass attenuation coefficient.

Table 8 Calculated mass attenuation coefficient and percentage difference among standard XCOM data with MCNPX, Geant4, and theoretical methods (%) of ovary and spleen

Nuclide	Mean-energy (MeV)	Mass attenuation coefficient of ovary				Percentage difference (%) for ovary		
		MCNP	GAENT4	Theoretical	XCOM	MCNP	GAENT4	Theoretical
Pd-103	0.021	0.74828	0.73239	0.73554	0.73840	1.338	0.813	0.387
I-125	0.029	0.40850	0.38551	0.39991	0.39970	2.201	3.55	0.052
Cs-131	0.030	0.38587	0.39254	0.37075	0.37960	1.651	3.408	2.331
Tc-99 m	0.140	0.15173	0.16729	0.15960	0.15290	0.765	9.411	4.381
Ba-133	0.218	0.13042	0.13253	0.13904	0.13220	1.346	0.249	5.173
Ir-192	0.380	0.10598	0.10720	0.10372	0.10760	1.505	0.371	3.605
Au-198	0.412	0.10020	0.10646	0.10355	0.10420	3.838	2.168	0.623
Cs-137	0.663	0.08502	0.09701	0.08139	0.08513	0.129	13.955	4.393
Ra-226	0.830	0.07703	0.08973	0.07532	0.07681	0.286	16.82	1.939
Co-60	1.25	0.06354	0.07183	0.06592	0.06283	1.13	14.324	4.918
Nuclide	Mean-energy (MeV)	Mass attenuation coefficient of spleen				Percentage difference (%) for spleen		
		MCNP	GAENT4	Theoretical	XCOM	MCNP	GAENT4	Theoretical
Pd-103	0.021	0.75267	0.75276	0.73715	0.74250	1.351	1.362	0.725
I-125	0.029	0.40881	0.38173	0.40537	0.40100	1.91	5.048	1.078
Cs-131	0.030	0.38711	0.39811	0.38624	0.38070	1.655	4.373	1.434
Tc-99 m	0.140	0.15114	0.15819	0.15091	0.15240	0.833	3.66	0.987
Ba-133	0.218	0.13022	0.14130	0.13012	0.13180	1.213	6.723	1.291
Ir-192	0.380	0.10645	0.10806	0.10376	0.10730	0.798	0.703	3.411
Au-198	0.412	0.10003	0.10447	0.10359	0.10390	3.868	0.545	0.299
Cs-137	0.663	0.08479	0.09626	0.08454	0.08484	0.0589	11.863	0.354
Ra-226	0.830	0.07544	0.08569	0.07656	0.07655	1.471	10.666	0.013
Co-60	1.25	0.06152	0.06317	0.06643	0.06261	1.771	0.886	5.75

4 Conclusion

The Monte Carlo method is a powerful tool for simulating the interaction of photons with the material, and one of its applications is to calculate the mass attenuation coefficient. The accuracy of this method depends on the simulated geometry, composition of the material, and density and use from the corrected physical model. This study proved that the MCNPX and Geant4 code are suitable and efficient codes for mass attenuation coefficients in low- and high-energy fields and can be beneficial for future studies, where experimental conditions and data are unavailable. The mass attenuation coefficients of human body organs were calculated using MCNPX, GEANT4, XCOM, and theoretical methods for the different medical sources within a photon energy range of 0.021–1.25 MeV and have used a standard simulation geometry. In this study, the data obtained from the Monte Carlo simulation for the standard deviation of mass attenuation coefficients simulated using the theoretical method and XCOM data were found to be extremely small, indicating that the results of the present investigation were in excellent agreement with the standard database. The discrepancy between the mass attenuation coefficients simulated using the Geant4 and theoretical methods and NIST data were found to be extremely small. The disparity between some of the results could be due to differences between the cross-sectional libraries of the Monte Carlo programs. The results of the present investigation into the Monte Carlo method were in excellent agreement with the standard database.

According to the results, the mass attenuation coefficient for cortical bone is higher due to its atomic number and higher density. Breast tissue has a lower mass attenuation coefficient than other organs because of its lower density. In addition, the results showed that, within the low photon energy range, the mass attenuation coefficient decreases with increasing energy, and within the higher energy range (1–2 MeV), the mass attenuation coefficients of the materials differ less and are almost equal.

Table 9 Calculated mass attenuation coefficient and percentage difference among standard XCOM data with MCNPX, Geant4, and theoretical methods (%) of muscle and cortical bone

Nuclide	Mean-energy (MeV)	Mass attenuation coefficient of muscle				Percentage difference (%) for muscle		
		MCNP	GAENT4	Theoretical	XCOM	MCNP	GAENT4	Theoretical
Pd-103	0.021	0.75216	0.73864	0.73794	0.73480	2.308	0.519	0.425
I-125	0.029	0.41131	0.39976	0.39903	0.39830	3.163	0.365	0.182
Cs-131	0.030	0.38842	0.38517	0.36152	0.37830	2.605	1.783	4.641
Tc-99 m	0.140	0.15305	0.16913	0.15910	0.15250	0.359	9.832	4.148
Ba-133	0.218	0.13101	0.13491	0.13869	0.13180	0.603	2.305	4.967
Ir-192	0.380	0.10689	0.10552	0.10372	0.10730	0.383	1.686	3.451
Au-198	0.412	0.10073	0.10759	0.10356	0.10390	3.147	3.429	0.328
Cs-137	0.663	0.08591	0.07351	0.08142	0.08491	1.164	15.508	4.286
Ra-226	0.830	0.07589	0.06854	0.07531	0.07660	0.935	11.759	1.712
Co-60	1.25	0.06268	0.06038	0.06575	0.06265	0.047	3.759	4.714
Nuclide	Mean-energy (MeV)	Mass attenuation coefficient of cortical bone				Percentage difference (%) for cortical bone		
		MCNP	GAENT4	Theoretical	XCOM	MCNP	GAENT4	Theoretical
Pd-103	0.021	3.97160	3.82857	3.46192	3.46000	12.881	9.626	0.055
I-125	0.029	1.70540	1.64494	1.49289	1.44100	15.503	12.398	3.475
Cs-131	0.030	1.54922	1.49721	1.39676	1.32000	14.795	11.836	5.495
Tc-99 m	0.140	0.14587	0.16152	0.16139	0.15280	4.75	5.398	5.322
Ba-133	0.218	0.12065	0.13845	0.12427	0.12630	4.682	8.775	1.633
Ir-192	0.380	0.11508	0.11009	0.10545	0.10120	12.061	8.075	4.03
Au-198	0.412	0.10691	0.10385	0.09134	0.09784	8.483	5.787	7.116
Cs-137	0.663	0.07824	0.09546	0.07190	0.07965	1.802	16.561	10.778
Ra-226	0.830	0.07082	0.08420	0.07373	0.07180	1.383	14.726	2.617
Co-60	1.25	0.05754	0.04501	0.05366	0.05869	1.998	30.393	9.373

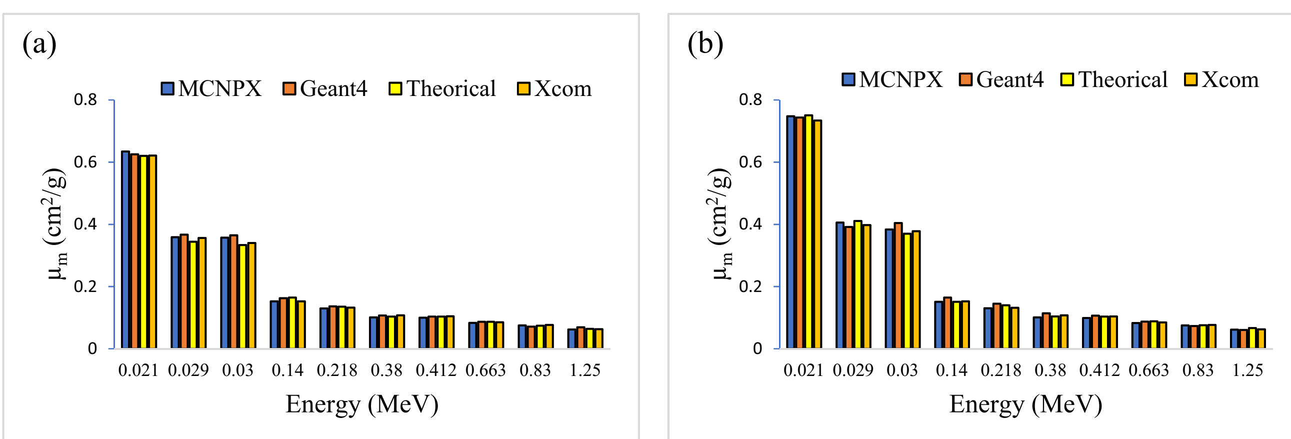

Fig. 3 (Color online) Mass attenuation coefficient for **a** breast and **b** blood

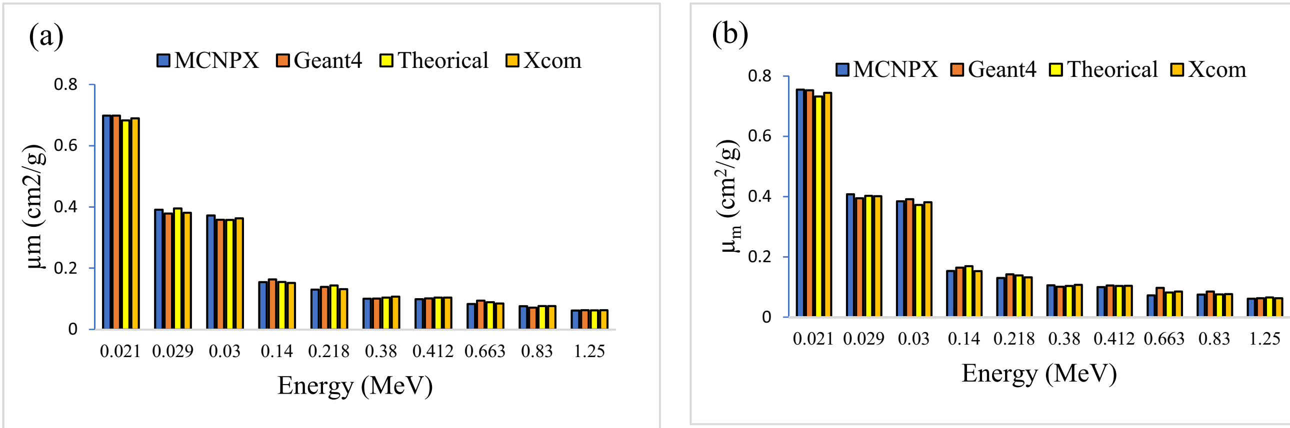

Fig. 4 (Color online) Mass attenuation coefficient for **a** skin and **b** lung

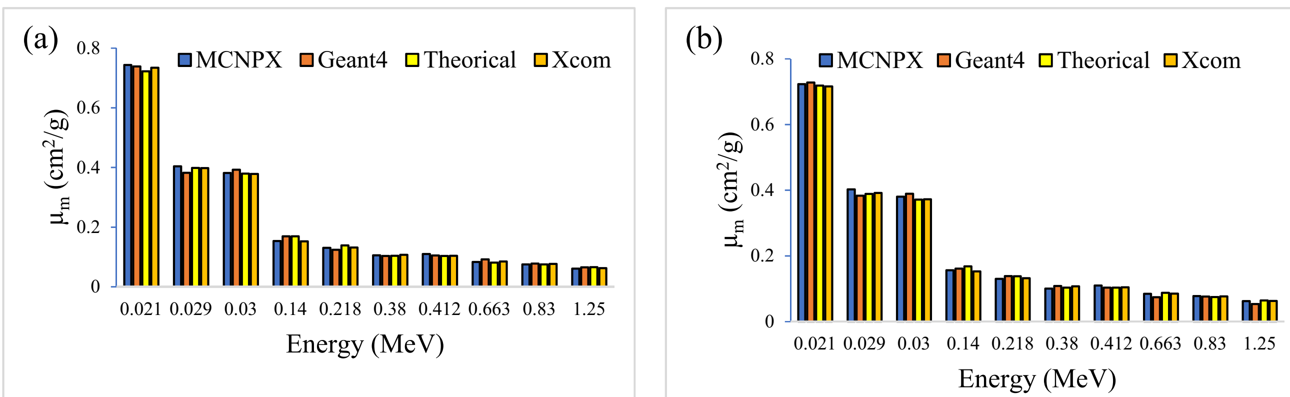

Fig. 5 (Color online) Mass attenuation coefficient for **a** kidneys and **b** pancreas

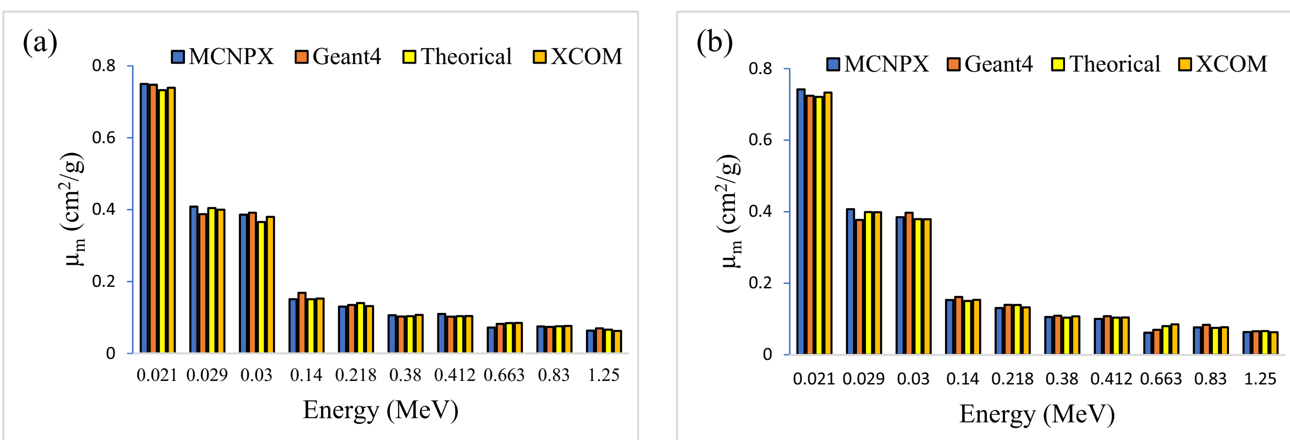

Fig. 6 (Color online) Mass attenuation coefficient for **a** liver and **b** thyroid

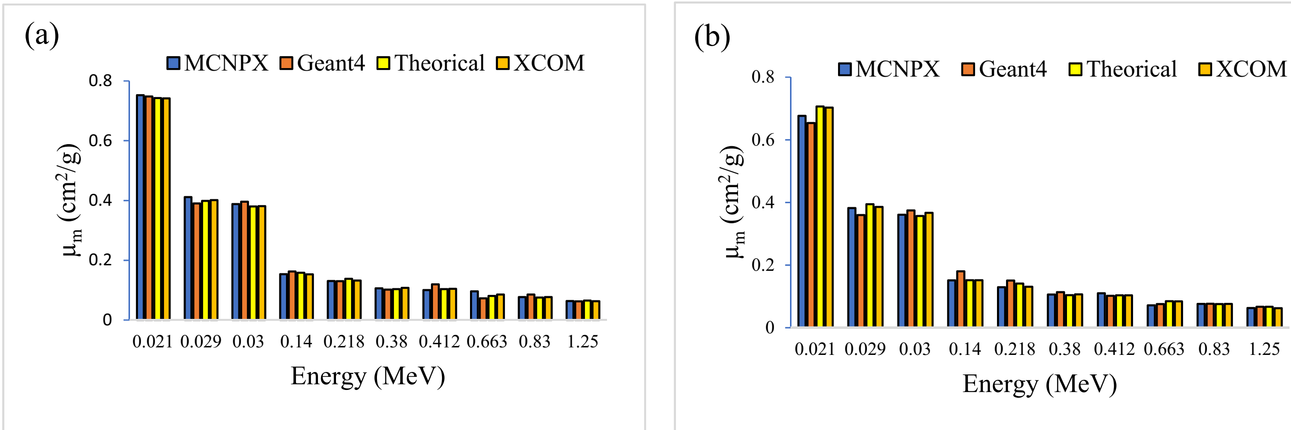

Fig. 7 (Color online) Mass attenuation coefficient for **a** brain and **b** eye lens

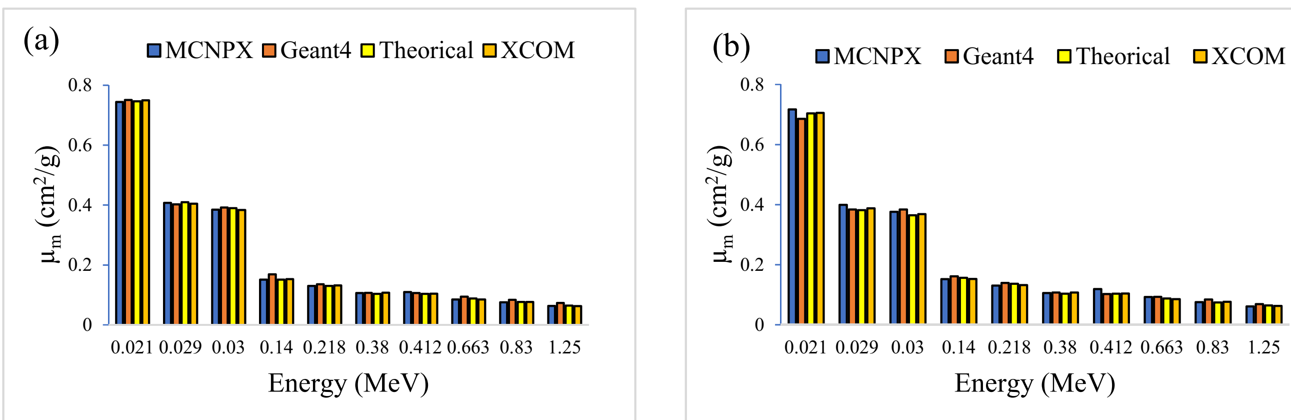

Fig. 8 (Color online) Mass attenuation coefficient for **a** heart and **b** large intestine

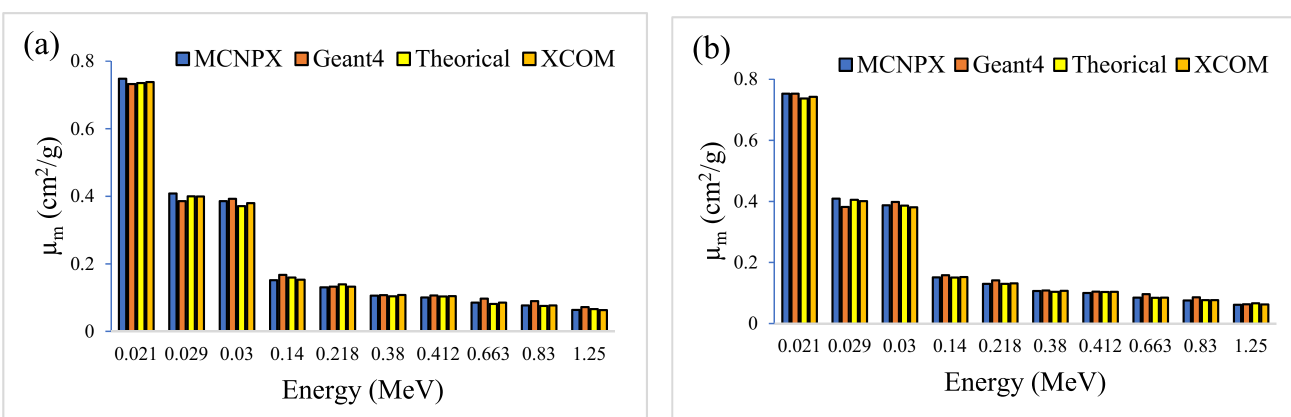

Fig. 9 (Color online) Mass attenuation coefficient for **a** ovary and **b** spleen

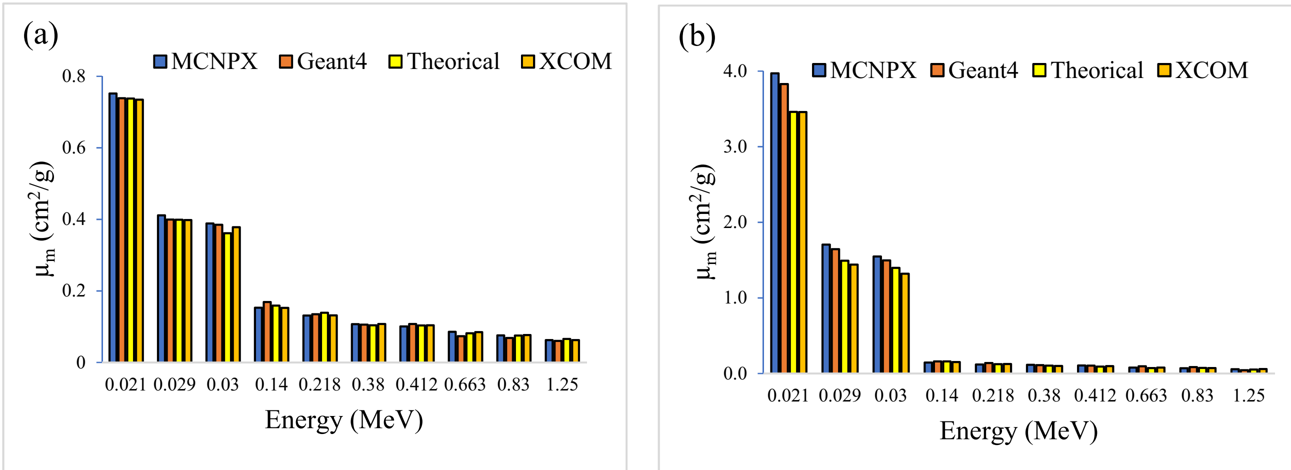

Fig. 10 (Color online) Mass attenuation coefficient for **a** muscle and **b** cortical bone

References

1. A.C. Moreno, R.J. Kudchadker, J. Wang et al., MRI image-guided low-dose rate brachytherapy for prostate cancer, in *Handbook of image-guided brachytherapy*. ed. by J. Mayadev, S. Benedict, M. Kamrava (Springer, Cham, 2017). https://doi.org/10.1007/978-3-319-44827-5_12
2. J.C. Blasko, P.D. Grimm, J.E. Sylvester et al., Palladium-103 brachytherapy for prostate carcinoma. Int. J. Radiat. Oncol. Biol. Phys. **46**, 839–850 (2000). https://doi.org/10.1016/S0360-3016(99)00499-X
3. T.L. Fowler, M.K. Buyyounouski, C.H. Jenkins et al., Clinical implementation of 3D printing for brachytherapy: techniques and emerging applications. Brachytherapy **15**, S166 (2016). https://doi.org/10.1016/j.brachy.2016.04.297
4. E.A. Markelova, S.S. Khujaev, A. Vasidov, The calculation of barium-131 radioactivity and obtaining the cesium-131 from barium-131 at Nuclear Reactor. Uzbekiston Fizika Zhurnali **13**, 381–386 (2011). http://inis.iaea.org/search/search.aspx?orig_q=RN:44048651
5. M. Fragoso, P.A. Love, F.V. Erhaegen et al., The dose distribution of low dose rate Cs-137 in intracavitary brachytherapy: comparison of Monte Carlo simulation, treatment planning calculation and polymer gel measurement. Phys. Med. Biol. **49**, 5459–5474 (2004). https://doi.org/10.1088/0031-9155/49/24/005
6. F. Issa, A.A. Rahman, R.P. Hugtenburg et al., Establishment of Ge-doped optical fibers as thermoluminescence dosimeters for brachytherapy. Appli. Radiat. Isot. **70**, 1158–1161 (2012). https://doi.org/10.1016/j.apradiso.2011.12.027
7. M.G. David, C. Salata, P.H. Rosado, et al., Determination of the chemical yield on the Fricke dosimetry for 192Ir sources used in brachytherapy. Braz. Cong.r Metrol. (2015). http://hdl.handle.net/2050011876/943
8. M.E. Alden, M. Mohiuddin, The impact of radiation dose in combined external beam and intraluminal Ir-192 brachytherapy for bile duct cancer. Int. J. Radiat. Oncol. Biol. Phys. **28**, 945–951 (1994). https://doi.org/10.1016/0360-3016(94)90115-5
9. IEl. Gamal, C. Cojocaru, E. Mainegra-Hing et al., The fricke dosimeter as an absorbed dose to water primary standard for Ir-192 brachytherapy. Phys. Med. Biol. **60**, 4481–4495 (2015)
10. E.C. Merchan, M. Magallon, J. Martin-Villar et al., Long term follows up of hemophilic arthropathy treated by Au-198 radiation synovectomy. Int. Orthop. **17**, 120–124 (1993). https://doi.org/10.1007/BF00183554
11. J. Dybicki, O.J. Balchum, G.R. Meneely et al., Treatment of pleural and peritoneal effusion with intracavitary colloidal radiogold (Au 198). AMA Arch. Intern. Med. **104**, 802–815 (1959). https://doi.org/10.1001/archinte.1959.00270110122017
12. M.I. Sayyed, F. Akman, I.H. Geçibesler et al., Measurement of mass attenuation coefficients, effective atomic numbers, and electron densities for different parts of medicinal aromatic plants in low-energy region. Nucl. Sci. Tech. **29**, 144 (2018). https://doi.org/10.1007/s41365-018-0475-0
13. A. Bagulya, J.M. Brown, H. Burkhardt et al., Recent progress of GEANT4 electromagnetic physics for LHC and other applications. J. Phys. Conf. Ser. **898**, 042032 (2017). https://doi.org/10.1088/1742-6596/898/4/042032
14. J.L. Venselaar, P.H. Van der Giessen, W.J. Dries, Measurement and calculation of the dose at large distances from brachytherapy sources: Cs-137, Ir-192, and Co-60. Med. Phys. **23**, 537–543 (1996). https://doi.org/10.1118/1.597811
15. G. Kemikiler, History of brachytherapy. Turk. J. Oncol. **34**, 1–10 (2019). https://doi.org/10.5505/tjo.2019.1
16. R.J. Gibbons, Myocardial perfusion imaging. Heart **83**, 355–360 (2000). https://doi.org/10.1136/heart.83.3.355
17. C.P. Goddard, A.H. Stead, P.A. Mason et al., An iodine-125 radioimmunoassay for the direct detection of benzodiazepines in blood and urine. Analyst **111**, 525–529 (1986). https://doi.org/10.1039/AN9861100525
18. M.R. Ioan, V. Fugaru, S. Bercea, et al., Co-60 Specific gamma-ray constant (Γ) determinations for various biological materials involved in radiotherapy procedures, by using GEANT4 and NIST XCOM. Rom. J. Phys., **63**, 701 (2018). https://www.researchgate.net/publication/319442968
19. E.E. Ermis, F.B. Pilicer, E. Pilicer et al., A comprehensive study for mass attenuation coefficients of different parts of the human body through Monte Carlo methods. Nucl. Sci. Tech. **27**, 54 (2016). https://doi.org/10.1007/s41365-016-0053-2
20. M.S. Al-Buriahi, H. Arslan, B.T. Tonguç, Mass attenuation coefficients, water, and tissue equivalence properties of some tissues by Geant4, XCOM, and experimental data. IJPAP. **57**, 433–437 (2019). http://op.niscair.res.in/index.php/IJPAP/article/view/22878/465477021
21. H.C. Manjunatha, L. Seenappa, Pocket formula for mass attenuation coefficient, effective atomic number, and electron density of human tissues. Nucl. Sci. Tech. **30**, 36 (2019). https://doi.org/10.1007/s41365-019-0565-7

22. A.H. Taqi, H.J. Khalil, Experimental, and theoretical investigation of gamma attenuation of building materials. J. Nucl. Part. Phys. **7**, 6–13 (2017). https://doi.org/10.5923/j.jnpp.20170701.02
23. H. Arslan, Photon attenuation parameters for some tissues from Geant4 simulation, theoretical calculations, and experimental data a comparative study. Nucl. Sci. Tech. **30**, 96 (2019). https://doi.org/10.1007/s41365-019-0617-z
24. B. Ababneh, R. Hashim, I.L. Shuaib, Investigation of mass attenuation coefficient of almond gum bonded *Rhizophora* spp. particleboard as equivalent human tissue using XRF technique in the 16.6–25.3 keV photon energy. Aust. Phys. Eng. Sci. Med. **39**, 871–876 (2016)
25. M. Alssabbagh, A.A. Tajuddin, M.B. Manap, et al., Evaluation of nine 3D printing materials as tissue-equivalent materials in terms of mass attenuation coefficient and mass density. Int. J. Adv. Appl. Sci. **4**, 168–173 (2017). https://www.researchgate.net/publication/321823909
26. A.M. El-Khayatt, A.M. Ali, V.P. Singh et al., Determination of mass attenuation coefficient of low-Z dosimetric materials. Radiat. Eff. Defects Solids **169**, 1038–1044 (2014). https://doi.org/10.1080/10420150.2014.988626
27. D.R. White, J. Booz, R.V. Griffith et al., Report 44. J. Int. Comm. Radiat. Units Meas. **os23**, NP (1989). https://doi.org/10.1093/jicru/os23.1.Report44
28. Y.S. Rammah, A.S. Abouhaswa, A.H. Salama et al., Optical, magnetic characterization, and gamma-ray interactions for borate glasses using XCOM program. J. Theor. Appl. Phys. **13**, 155–164 (2019). https://doi.org/10.1007/s40094-019-0331-6
29. J.H. Hubbell, Photon cross-section, attenuation coefficient, and energy absorption coefficients from 10 keV to 100 GeV. National Bureau of Standards Report NSRDS-NBS29, Washington, DC (1969).
30. G. Lakshminarayana, M.I. Sayyed, S.O. Baki et al., Borotellurite glasses for gamma-ray shielding: an exploration of photon attenuation coefficients and structural and thermal properties. J. Electron. Mater. **48**, 930–941 (2019). https://doi.org/10.1007/s11664-018-6810-8
31. V.P. Singh, S.P. Shirmardi, M.E. Medhat et al., Determination of mass attenuation coefficient for some polymers using Monte Carlo simulation. Vacuum **119**, 284–288 (2015). https://doi.org/10.1016/j.vacuum.2015.06.006
32. H.O. Tekin, E.E. Altunsoy, T. Manici et al., Mass attenuation coefficients of human body organs using MCNPX Monte Carlo code. Iran. J. Med. Phys. **14**, 229–240 (2017). https://doi.org/10.22038/IJMP.2017.23478.1230
33. A. Bagulya, J.M. Brown, H. Burkhardt et al., Recent progress of GEANT4 electromagnetic physics for LHC and other applications. J. Phys. Conf. Ser. **898**, 042032 (2017). https://doi.org/10.1088/1742-6596/898/4/042032
34. K. Özge, H.O. Tekin, V.P. Singh, Determination of mass attenuation coefficients of different types of concretes using Monte Carlo method. EJOSAT **15**, 591–598 (2019). https://doi.org/10.31590/ejosat.535203